MEMS Test Structures for Mechanical Characterization of VLSI Thin Films

David Herman[1], **Michael Gaitan**[2], and **Don DeVoe**[1]

[1]Department of Mechanical Engineering
University of Maryland
College Park, MD 20742

[2]Electronics & Electrical Engineering Laboratory
National Institute of Standards and Technology
Gaithersburg, MD 20899

Abstract

As the number of layers for interconnects increases in an integrated circuit, reliability becomes increasingly dependent on mechanical properties such as elastic modulus and residual stress. A method for determining the Young's modulus of each film in a fully processed integrated circuit is presented. This method utilizes MEMS-based cantilever test structures prepared using standard silicon micromachining techniques. The multi-layer cantilevers are excited using mechanical excitation and resonance is detected using laser interferometry. The resonant frequencies of the cantilevers can then be utilized in a composite beam model to extract the Young's modulus for each layer.

I. Introduction

Residual stresses in and between the layers of an IC develop during processing and arise from a combination of mismatched thermal expansion coefficients and intermolecular forces. These residual stresses heighten the probability of stress-related failures due to mechanisms such as electromigration, stress migration, and delamination [1].

The residual stress in an IC is usually measured indirectly by measuring the residual strain of a given thin film using wafer curvature measurements and multiplying it by a value for Young's modulus. However, Young's modulus for the thin films in an IC can vary from process to process. An easily executed method for determining the local Young's modulus is needed to accurately determine the stress in the layers of a processed IC.

Previously, Petersen and Guarnieri have used electrostatically vibrated cantilever beams to study the Young's modulus of thin deposited films [2]. The technique is useful for comparing thin film properties to published bulk material properties, but would be difficult to implement in a VLSI process. Kiesewetter et al implemented mechanical excitation to determine the Young's modulus of single-layer silicon nitride films [3]. However, the single-layer structures that they used are not feasible for determining the properties of multiple layers in an IC.

The method of mechanically exciting cantilevers and using laser interferometry to detect resonance has two primary advantages over previous methods. The MEMS-based structures are CMOS process compatible, meaning they can be produced on-chip. Additionally, the use of combinations of multi-layer structures enables the modulus of elasticity to be determined for all films in a fully processed IC.

In this paper, multi-layer MEMS-based CMOS process compatible cantilever test structures were excited to resonance using mechanical excitation. The resonant frequencies were then used in a composite beam model to extract the modulus of elasticity for each material in the test structures.

II. Theoretical Background

The natural frequency for the free undamped vibration of a uniform cantilever is a function of its cross-sectional properties, length, and boundary conditions only, and is defined as [4],

$$f = \frac{\lambda^2}{2\pi}\sqrt{\frac{EI}{mL^4}} \tag{1}$$

where E, I, m, and L are the Young's modulus, area moment of inertia about the neutral axis, mass per unit length, and length of the cantilever, respectively. The product of the Young's modulus with the moment of inertia (EI) is defined as the bending stiffness. The symbol λ represents the eigenvalue corresponding to the resonance mode number and boundary conditions of the cantilever. For a fixed-free cantilever in its first mode of vibration, $\lambda = 1.875$.

The natural frequency for the free undamped vibration of a composite cantilever can be found by replacing the bending stiffness (EI) and mass per unit length (m) terms with composite bending stiffness ($\overline{EI}$) and composite mass per unit length ($\overline{m}$). These terms are defined as [1],

$$\overline{EI} = \sum_{i=1}^{N} E_i I_i \quad , \quad \overline{m} = \sum_{i=1}^{N} m_i \qquad (2),(3)$$

where N is the number of layers in the composite cantilever and m_i is the mass per unit length of the i^{th} layer in the cross section of the cantilever.

Substituting equations (2) and (3) into equation (1) and squaring the resulting equation yields an equation for the natural frequency squared of a cantilever as a function of the properties of its layers.

$$f^2 = \left(\frac{1.875^2}{2\pi}\right)^2 \frac{\sum_{i=1}^{N} E_i I_i}{L^4 \sum_{i=1}^{N} m_i} \qquad (4)$$

It should be noted that the E term in equations (1) and (4) is only equivalent to the true Young's modulus if uniaxial strain in the cantilever is assumed. Otherwise this term corresponds to the effective modulus of elasticity of the beam. If the beam is assumed to be thin (height << width), slender (width << length), and isotropic, the effective modulus of elasticity is given by $E(1-\nu^2)$, where ν is the Poisson's ratio of the cantilever material. For the remainder of this paper, E or Young's modulus will refer to the effective modulus of elasticity. Because Poisson's ratio is relatively small for each of the materials in the test structures, the difference between the effective modulus and true modulus will be not be substantial.

If viscous damping due to air is neglected, then the measured resonant frequency is equal to the frequency given by the equation above. By finding the composite bending stiffnesses of a number of cantilevers of various compositions, the Young's modulus of the individual materials in the cantilevers can be calculated using an iterative approach described in the following.

III. Fixed-Free Cantilever Test Structures

Test structures were designed and fabricated to determine the modulus of elasticity of films in a multi-layer IC. The structures were fabricated in the 1.2 μm feature size, two-metal, two-polysilicon American Microsystems, Inc. (AMI) ABN process available through the MOSIS foundry service. Sixteen cantilevers of various compositions were created by either including or not including the following interconnect layers: poly-1, poly-2, metal-1, and metal-2, see Table 1. The cantilevers consist of thin polysilicon and aluminum interconnect layers encased in oxide with oxide layers sandwiched between each of the interconnect layers.

Arrays of sixteen cantilevers were designed with two different geometries; wide and narrow. The wide cantilevers were measured to be 439.2 μm long and 38.4 μm wide, see Figure 1. The narrow cantilevers were measured to be the same length (439.2 μm) and one half as wide (19.2 μm). The interconnect layers in the wide and narrow cantilevers are 32.4 μm and 13.2 μm wide, respectively. The cantilevers are bordered by 3 μm of oxide on each of the released edges and the interconnect layers in the cantilevers extend 50 μm past the attachment point of the cantilever on the unreleased edge.

Table 1. Cantilever layer combinations where each cantilever contains all oxide layers. P1, P2, M1, and M2 represent the first poly layer, second poly layer, first metal layer, and second metal layer, respectively.

Cantilever Combination Number	Included Interconnect Layers
1	None
2	P1
3	P2
4	P1 P2
5	M1
6	P1 M1
7	P2 M1
8	P1 P2 M1

Cantilever Combination Number	Included Interconnect Layers
9	M2
10	P1 M2
11	P2 M2
12	P1 P2 M2
13	M1 M2
14	P1 M1 M2
15	P2 M1 M2
16	P1 P2 M1 M2

Layer thicknesses were obtained from profilometer and SEM measurements. The thicknesses of the poly-1 and poly-2 layers were measured to be 0.33 μm. The thicknesses of the metal-1 and metal-2 layers were measured to be 0.75 μm and 1.06 μm, respectively.

The cantilever test structures were released using standard CMOS compatible silicon micromachining techniques. A pulsed xenon difluoride isotropic etching process was used on selected dies to remove the silicon beneath and around each cantilever. Other dies were etched with a tetramethylammonium hydroxide (TMAH) solution, see Figure 2. This anisotropically removed the silicon beneath and around each cantilever and undercut the attachment point evenly along a line perpendicular to the length of the cantilever.

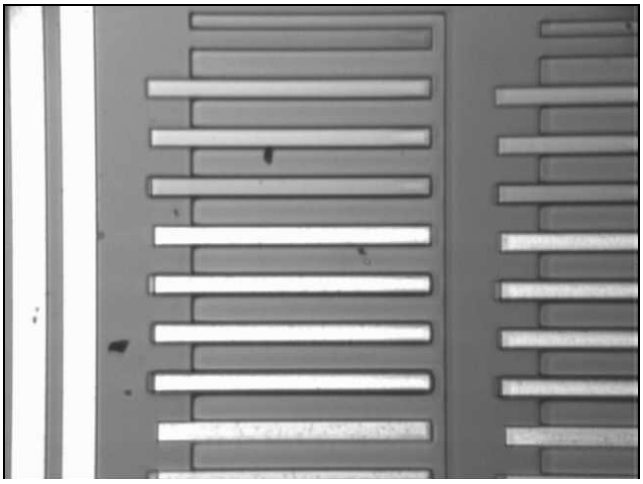

Fig. 1. Photograph of wide cantilevers prior to release. The cantilevers pictured correspond to cantilever combination numbers 1 through 10 from Table 1.

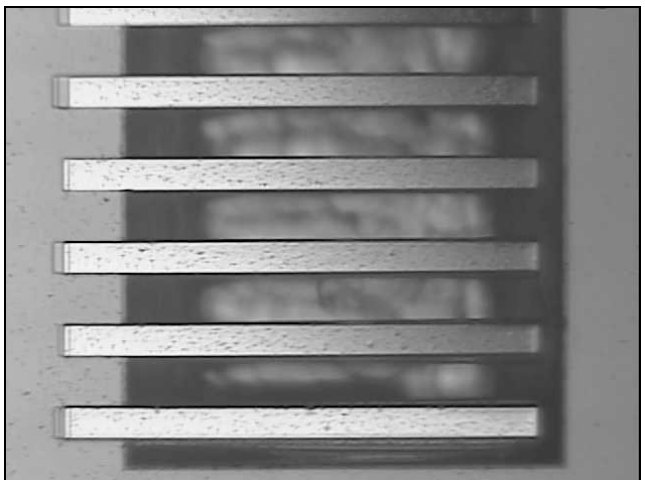

Fig. 2. Photograph of wide cantilevers after release with TMAH solution. The cantilevers pictured correspond to cantilever combination numbers 11 through 16 from Table 1.

IV. Technique for Determining Resonance

To excite the test structures, a small piezoelectric actuator was used. A function generator created sinusoidal signals that first passed through an amplifier and then were sent to the piezoelectric actuator. The actuator was attached to a microscope stage with double-sided tape and the test die was attached to the actuator with double-sided tape.

The displacement of each test cantilever was detected using a laser doppler vibrometer (LDV). The displacement signal was sent from the LDV controller to an oscilloscope. The resonant frequency of each cantilever was determined by sweeping through frequencies with the function generator, observing the amplitude of the waveform on the oscilloscope, and recording the frequency at which the first peak occurred. Using this method the resonant frequency of each cantilever was found and resolved to within ± 30 Hz or about 0.15% of the resonant frequency.

V. Model and Assumptions

Air damping is disregarded in the previous equations dealing with resonant frequency. The influence of damping can be quantified using the oscillating quality factor, *Q*. The relationship between *Q* and the measured resonant frequency is given by [3],

$$f_r = f_o \sqrt{1 - \frac{1}{4Q^2}} \tag{5}$$

where f_o is the undamped natural frequency and f_r is the measured natural frequency. For small values of damping, f_o and f_r are approximately equal.

Q-factors were determined experimentally using the half-power-point method [3];

$$Q = f_o / \Delta f_o \tag{6}$$

where f_o is the resonant frequency and Δf_o is the frequency bandwidth at the half-power point. Using the normalized frequency response plots in Figure 3 the *Q*-factors for the pure oxide cantilever and the cantilever containing poly-1, metal-1, and metal-2 were calculated to be 48 and 98, respectively. It is likely that these values are not accurate due to the poor resolution of the frequency response plot near resonance. Another method for determining *Q* is to define it as the peak value of the magnification function [5]. This method yielded a value of 21 and 24 for the *Q*-factors of the oxide and combination cantilevers, respectively.

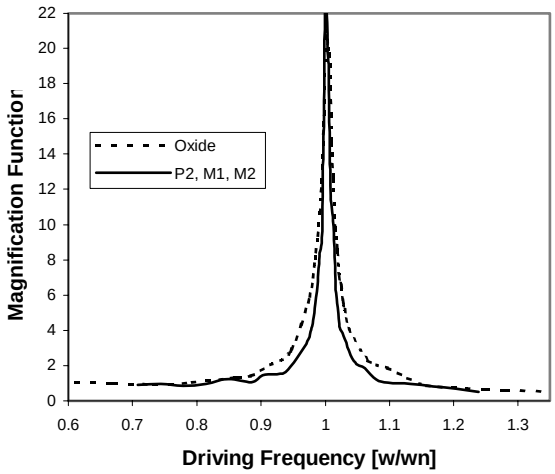

Fig. 3. Measured frequency response of two cantilevers: one comprised of only oxides, the other comprised of oxides, the second polysilicon layer, and both metal layers.

If *Q* is assumed to be at least 20 for each cantilever, the maximum deviation of the measured resonant frequency from the true resonant natural frequency is 0.03%. Therefore, air damping can be neglected when calculating Young's modulus from the measured resonant frequency of the test structures.

Another assumption implicit in the resonant frequency equations is that the cross section is uniform along the length of the cantilever. This assumption is primarily true along the entire length of the cantilever except at the released edge where there is an oxide border of 3 μm. At worst this has the effect of measuring the resonant frequency for a cantilever 3 μm shorter than estimated. This introduces an additional maximum error of 0.7% to the length of the cantilever. This error is small compared to that caused by undercutting at the base of the cantilever, and can therefore be neglected.

VI. Calculation of Young's Modulus

To determine the Young's modulus of each material in the test structures, equation (4) was converted to a matrix equation of the form,

$$\left[f^2\right] = \left(\frac{1.875^2}{2\pi L^2}\right)^2 \left[\frac{I}{\overline{m}}\right][E] \qquad (7)$$

where $[f^2]$ is a column vector of the squared resonant frequencies of different combination cantilevers and [*E*] is a column vector of the effective Young's modulus of each layer in the tested cantilevers.

When substituting measured values of resonant frequency in $[f^2]$ and trying to solve for [*E*], a problem arises due to the fact that the moment of inertia terms in $[I/\overline{m}]$ are a function of [*E*]. This problem is solved by using preliminary values of [*E*], [E_0], to calculate $[I/\overline{m}]$, solving for [*E*], and repeating the process after setting [E_0] equal to [*E*].

Estimated values of frequency can be calculated using equation (7) with [*E*] set equal to [E_0]. With each iteration the estimated values of resonant frequency approach the measured values. When the estimated frequencies equal the measured frequencies, [*E*] becomes stationary. If estimated frequency was plotted against measured frequency and a linear regression were performed, the resulting line would have a slope of one and an intercept of zero.

The convergence criteria was set so that when a linear regression is performed on the estimated frequency vs. measured frequency data points, the resulting line has a slope of 1 ± 0.02 and an intercept of ± 0.5 kHz. As can be seen in Figure 4, for the particular cantilevers tested, only two iterations were required before satisfying the convergence criteria. All other calculations of [*E*] based on other combinations of cantilevers behaved similarly and converged quickly.

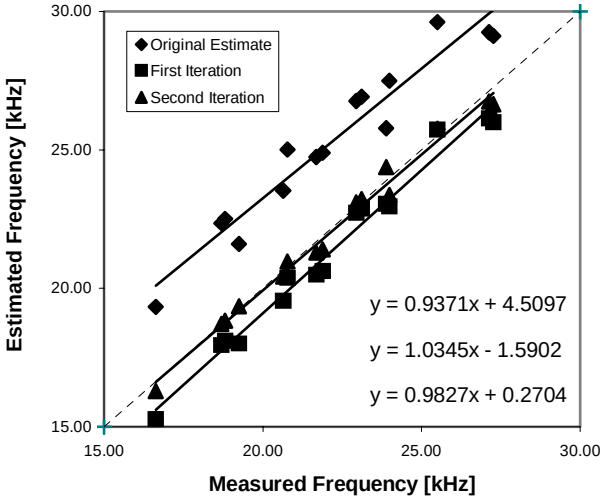

Fig. 4. Estimated frequency vs. measured frequency after 0, 1, and 2 iterations. The equations of the linear fit lines are displayed on the graph in the order corresponding to that of the legend.

VII. Results and Discussion

The resonant frequency of most of the cantilevers was determined using the method described in section IV. Because of problems such as cantilevers braking during release and particle contamination, it was impossible to use all combinations of cantilevers to calculate Young's modulus. However, various combinations of cantilevers could be used to calculate the Young's modulus for each material in the test structures.

The calculated values for Young's modulus were grouped by cantilever geometry and release method. The results can be seen in Figure 5.

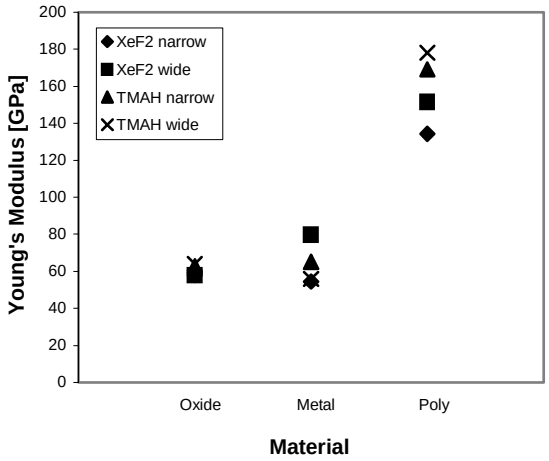

Fig. 5. Young's modulus of oxide, metal, and polysilicon layers in cantilevers. Data points are average values of data taken from narrow or wide cantilevers released in either xenon difluoride or a tetramethylammonium hydroxide solution.

Table 2 lists the average and standard deviation of the Young's modulus of each material obtained using the four combinations of cantilever geometry and release technique.

Table 2. Mean and standard deviation of Young's modulus for each material in the cantilevers.

	Mean	Standard Deviation
E_{oxide} [GPa]	60.71	3.26
E_{metal} [GPa]	63.84	11.60
E_{poly} [GPa]	158.27	19.43

The average values of the Young's modulus for each material are in fair agreement with the text values [1,6] of 72 GPa, 69 GPa, and 162 GPa for silicon dioxide, aluminum, and polysilicon, respectively. However, the standard deviations in the calculated values are a cause of concern. The standard deviation of the oxide modulus is reasonable at close to 5% of the mean, but the standard deviations of the moduli of the metal and polysilicon layers are considerably larger at 18% and 12% of their respective means.

There are a number of factors that could be responsible for the large standard deviations. The most likely cause of error is uncertainty in the values for layer thicknesses. This is because Young's modulus and the moment of inertia are of the same order in the frequency equation and the moment of inertia is proportional to the layer thickness cubed.

Because the test structures were fabricated through a commercial service, layer thickness information was not available. Thickness values based on profilometer and SEM measurements seem reasonable, but the accuracy of the thickness values obtained through these measurements is questionable, particularly for the oxide layers. If this technique for determining Young's modulus were implemented by an IC manufacturer, the layer thicknesses would be known precisely and the results of the technique would undoubtedly be more accurate. Future plans include the fabrication of a structure that will enable the thickness of each layer to be extracted from a simple profilometer measurement.

Another cause of the wide range of values of Young's modulus is uncertainty regarding the boundary conditions and the lengths of the cantilevers. Young's modulus is calculated assuming that the cantilever is free at one end and fixed at the other. However, due to undercutting of the attachment point during etching, the boundary condition at the attachment point of the cantilever is not quite fixed. This undercutting also increases the effective length of the cantilever by some uncertain amount.

Anisotropic etching was found to yield a better boundary at the attachment point than isotropic etching, but undercutting of the oxides near the cantilever attachment point is still a problem. A combination of isotropic and anisotropic etching will be used in the future in hopes of obtaining a boundary condition that more closely resembles a fixed boundary.

Fabricating and testing cantilevers of various lengths would help to minimize error in the length of the cantilevers. The length term can be factored out of the frequency equation. The remaining terms would be equal to the slope of the line created by plotting frequency with respect to one over length squared. Using linear regression with cantilevers of different lengths would introduce less error than using a single value for the length of the cantilevers.

One final source of error is related to the geometry of the cross section of the cantilevers. When calculating the areas and moments of inertia of the layers in the cross section, it was assumed that the layers are in the shape of rectangles stacked upon each other. The error due to this assumption is more substantial in narrower cantilevers where the overlap of oxides at the edges of the cross section is a more substantial portion of the entire width of the cross section.

One way of reducing this error would be to better model the geometry of the cross section. Another method would be to increase the width of the cantilever so that the effect of the edges becomes negligible. However, if the cantilevers are too wide, the residual compressive stresses in the cantilever will cause it to wrinkle at the attachment point [2].

VIII. Conclusion

The method of using mechanical excitation and optical detection of resonance of multi-layer cantilevers is a simple way of determining the Young's modulus of individual films in a processed IC. In this paper, the technique was validated and the average values for Young's modulus of silicon dioxide, aluminum, and polysilicon were found to be 60.71 $\pm$ 3.26 GPa, 63.84 $\pm$ 11.60 GPa, and 158.27 $\pm$ 19.43 GPa, respectively.

Acknowledgement

This work was supported by the NIST Office of Microelectronic Programs.

References

[1] Smee, S. A., Gaitan, M., Novotny, D. B., Joshi, Y., and Blackburn, D. L., *IC Test Structures for Multi-Layer Stress Determination*, IEEE Electron Device Letters, Vol. 21, No. 1, pp. 12-14, 2000.

[2] Petersen, K. E., Guarnieri, C. R., *Young's modulus measurements of thin films using micromechanics*, J. Appl. Phys., Vol. 50, No. 11, pp. 6761-6766, 1979.

[3] Kiesewetter, L., Zhang, J.-M., Houdeau, D., Steckenborn, A., *Determination of Young's moduli of micromechanical think films using the resonance method*, Sensors and Actuators A, Vol. 35, pp. 153-159, 1992.

[4] Beards, C. F., *Structural Vibration Analysis*, Wiley, New York, p. 28, 1983.

[5] Meirovitch, L., *Fundamentals of Vibrations*, McGraw Hill, New York, p. 116, 2001.

[6] Elbrecht, L., Storm, U., Catanescu, R., Binder, J., *Comparison of stress measurement techniques in surface micromachining*, J. Micromech. Microeng, Vol. 7, pp. 151-154, 1997.